

FastTrackTr: Towards Fast Multi-Object Tracking with Transformers

Liao Pan, Yang Feng*, Wu Di, Yu Jinwen, Zhao Wenhui, Liu Bo

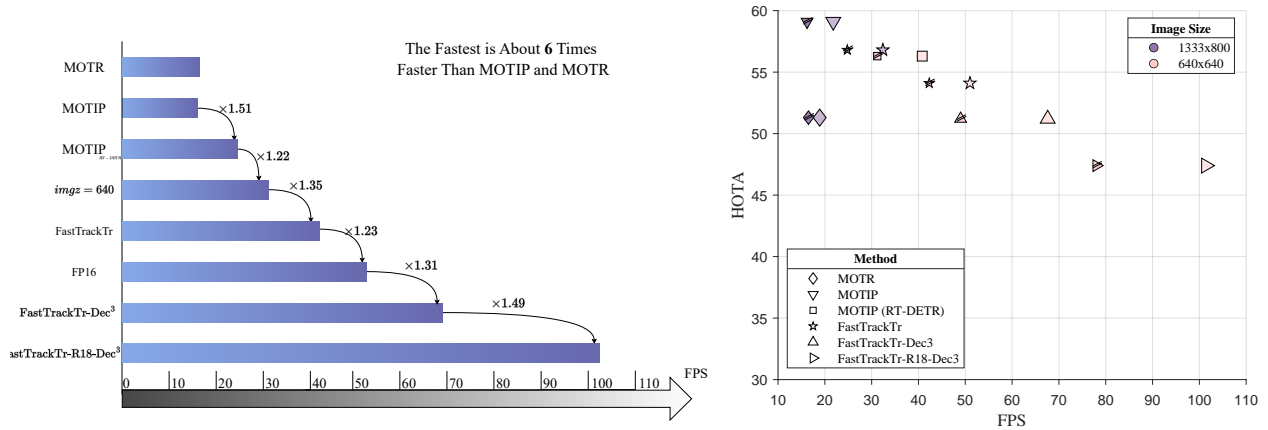


Figure 1. A comparison of the FPS and HOTA of various versions of FastTrackTr and the most advanced transformer-based models on a single NVIDIA 4090. The numerical precision marked with diagonal lines in the right figure is FP32, while that without lines is FP16.

Abstract

Transformer-based multi-object tracking (MOT) methods have captured the attention of many researchers in recent years. However, these models often suffer from slow inference speeds due to their structure or other issues. To address this problem, we revisited the Joint Detection and Tracking (JDT) method by looking back at past approaches. By integrating the original JDT approach with some advanced theories, this paper employs an efficient method of information transfer between frames on the DETR, constructing a fast and novel JDT-type MOT framework: FastTrackTr. Thanks to the superiority of this information transfer method, our approach not only reduces the number of queries required during tracking but also avoids the excessive introduction of network structures, ensuring model simplicity. Experimental results indicate that our method has the potential to achieve real-time tracking and exhibits competitive tracking accuracy across multiple datasets.

Liao Pan, Yang Feng, Wu Di, Yu Jinwen, Zhao Wenhui and Liu Bo are with Key Laboratory of Information Fusion, School of Automation, Northwestern Polytechnical University, Xi'an, China. (e-mail: liaopan@mail.nwpu.edu.cn, yangfeng@nwpu.edu.cn, wu_di821@mail.nwpu.edu.cn, yujinwen@mail.nwpu.edu.cn, zwh2024202513@mail.nwpu.edu.cn, 503790475@qq.com)

1. Introduction

Multi-object tracking (MOT) has long been a computer vision task of great interest to researchers and developers, with extensive application prospects across various industries. Currently, the mainstream tracking models are primarily online models, and the paradigm that has garnered widespread attention in recent years within online models remains tracking-by-detection (TBD). This paradigm, originating from SORT [1], has stood the test of time and demonstrates remarkable vitality. Its improved derivative methods [7, 19, 41] continue to be considered state-of-the-art (SOTA).

In recent years, some tracking methods based on transformer [34] have also attracted considerable attention. However, these methods [10, 11, 20, 31, 39, 42, 43] face a significant challenge: suboptimal inference speed. There are various reasons for this, such as the slow performance of the MOTR series, which relies on query-based tracking. The main reason is not the network structure, but issues related to hardware acceleration caused by the variable number of queries (detailed justification can be found in the appendix). Both our experiments and other works [22] have also demonstrated that the inference speed after lightening the network is still not very ideal. Regarding another recent method, MOTIP [11], while it addresses many of MOTR's issues, its main problem lies in its complex network struc-

ture. Even after replacing MOTIP’s Deformable DETR [51] with RT-DETR [48], its inference speed remains unsatisfactory (results shown in Figure 1).

Methods following the tracking-by-detection paradigm often claim to be extremely fast, but in reality, aside from those purely based on kinematics [3], the speed of most MOT systems is not ideal once the time required for the detection model is considered. Purely kinematic models typically perform worse than when they are combined with reid networks. So, is there a way to achieve both fast and accurate tracking? To address this question, we must look back at the JDT (Joint Detection and Tracking) paradigm, which was initially renowned for its speed. Although it has fallen out of favor in recent years due to various reasons, it likely represents a solution to the aforementioned issues. Previously, there was a transformer-based JDT model, known as the TransTrack [31], which shares the same pain points as MOTIP, including having two decoders. Other methods [2, 20, 38], similar to MOTR, track based on queries. CNN-based JDT models [35, 45], on the other hand, typically produce detection results and their corresponding id embeddings for association matching, with their main issue being that the models are outdated, hence they do not keep pace with current standards.

Based on the above discussion, we present **FastTrackTr**, a **Fast** multi-object **Tracking** method grounded in the **Transformer** architecture and aligned with the JDT paradigm. This tracking method achieves impressive tracking progress through a unique decoder that integrates past information. Additionally, due to the ease of generating masks for this method, the batch size can be set relatively large, making our model considerably more training-friendly compared to some of the latest transformer-based MOT methods. Additionally, due to the ease of generating masks for this method, the batch size can be set relatively large, making our model considerably more training-friendly compared to some of the latest transformer-based MOT methods.

Furthermore, it is noteworthy that models with a single decoder are capable of achieving end-to-end tracking without increasing the number of queries. This point is further discussed in the subsequent sections and the [appendix](#) of this document.

In summary, the main innovations of this paper are as follows:

- 1) proposing **FastTrackTr**, a novel transformer-based MOT method that achieves fast inference speed while maintaining high accuracy.
- 2) introducing a cross-decoder mechanism that implicitly integrates historical trajectory information, eliminating the need for additional queries or decoders.
- 3) Extensive experiments on multiple benchmark datasets, including DanceTrack [32], SportsMOT [6] and MOT17

[21], demonstrate that our model not only achieves competitive accuracy SOTA methods, but also significantly improves inference speed.

2. Related work

2.1. Transformer-based MOT Methods

The earliest Transformer-based MOT methods were TransTrack [31] and TrackFormer [20]. The former is a JDT model, while the latter introduced the concept of track queries, utilizing these special queries to achieve tracking.

Subsequently, MOTR [43] proposed tracklet-aware label assignment (TALA), which optimized label assignment during the training phase to achieve end-to-end tracking. Later improvements to MOTR, such as MOTRv2 [47], MeMOTR [10], MOTRv3 [42], and CO-MOT [39], demonstrated the powerful tracking performance of the MOTR paradigm. Some efforts have been made to address MOTR’s slow inference speed through model lightweighting, but the results have been less than ideal. Recently, alternative Transformer architectures have been proposed. MOTIP’s [11] novel approach of directly predicting tracked object ID numbers is refreshing, while PuTR’s [14] use of Transformers to directly construct a tracking-by-detection paradigm tracker has also been inspirational.

2.2. Tracking-by-Detection

The TBD paradigm can be considered one of the simplest and most practical tracking methods. Since it essentially associates detected targets, this class of methods often yields satisfactory tracking accuracy as long as the detection results are not poor.

The initial SORT algorithm simply utilized the motion state of detected objects for association. Subsequent models like DeepSORT [36] and ByteTrack [46] improved tracking accuracy by enhancing detection precision and employing embedding-based Re-identification (Re-id) networks. Some approaches, like OC-SORT [3] and HybridSORT [41], improved upon SORT using purely kinematics-based methods. Later models such as MotionTrack [24], DeepOC-SORT [19], and SparseTrack [16] demonstrated that simultaneous improvements in both Re-id network utilization and kinematic models yield the most significant performance enhancements.

Currently, there are also algorithms that directly use networks for association. Besides the aforementioned PuTR [14], SUSHI [5] is a tracking method based on graph neural networks.

2.3. Joint Detection and Tracking

Joint detection and tracking aims to achieve detection and tracking simultaneously in a single stage. This approach was common a few years ago but has been seen less fre-

quently in recent years. Here, we briefly review its development history. D&T [8] first proposed a multi-task architecture based on frame-based object detection and cross-frame trajectory regression. Subsequently, Integrated-Detection [52] improved detection performance by combining detection bounding boxes in the current frame with trajectories from the previous frame. Tracktor [30] directly used tracking boxes from the previous frame as candidate regions, then applied bounding box regression to provide tracking boxes for the current step, thus eliminating the box association process. JDE [35] and FairMOT [45] learned object detection and appearance embedding tasks from a shared backbone network. CenterTrack [49] localized targets through tracking-conditioned detection and predicted their offsets from the previous frame. TransTrack used two decoders to handle tracking and detection separately, then matched and associated the results from both decoders. Our FastTrackTr, by introducing a novel decoder, returns to the essence of the JDT method, simplifies the network structure, and achieves fast tracking.

3. Method

3.1. FastTrackTr Architecture

The overall structure of FastTrackTr is illustrated in Figure 2. In frame T_1 , a standard decoder is used to initialize the initial historical information. Subsequently, in the following frames, a Historical Encoder is employed to initialize this historical-representative information. In the next frame, a Historical Decoder, which includes an additional cross-attention layer compared to normal decoder layers, processes this historical information. The tracking principle is very similar to that of JDT and FairMOT, utilizing an additional ID Embedding head to obtain the object’s appearance embedding, which is then used along with detection results for association and matching. It is worth noting that the backbone network is ResNet [13].

3.2. Learning Detection and ID Embedding

To enable our FastTrackTr to simultaneously output both the target’s position and appearance embedding in a single forward pass, we formulate the problem as follows: Suppose we have a training dataset $\mathbf{I}, \mathbf{B}, \mathbf{y}_{i=1}^N$. Here, $\mathbf{I} \in \mathbb{R}^{c \times h \times w}$ represents an image frame, and $\mathbf{B} \in \mathbb{R}^{k \times 4}$ denotes the bounding box annotations for the k targets in this frame. $\mathbf{y} \in \mathbb{Z}^k$ represents the partially annotated identity labels, where -1 indicates targets without an identity label. We hope model can output predicted bounding boxes $\hat{\mathbf{B}} \in \mathbb{R}^{\hat{k} \times 4}$ and appearance embeddings $\hat{\mathbf{F}} \in \mathbb{R}^{\hat{k} \times D}$, where D is the dimension of the embedding.

For the output box, this requirement is easily met, as DETR[4] itself is a detection model. To achieve rapid performance, this paper employs RT-DETR [48] as the base

model, which inherently possesses state-of-the-art detection capabilities. We have not made significant modifications to its detection component. The loss function for this part remains consistent with RT-DETR, as shown below:

$$\begin{aligned} \mathcal{L}_{det} = \mathcal{L}(\hat{y}, y) &= \mathcal{L}_{box}(\hat{b}, b) + \mathcal{L}_{cls}(\hat{c}, \hat{b}, y, b) \\ &= \mathcal{L}_{box}(\hat{b}, b) + \mathcal{L}_{cls}(\hat{c}, c, IoU) \end{aligned} \quad (1)$$

where \hat{y} and y denote prediction and ground truth, $\hat{y} = \{\hat{c}, \hat{b}\}$ and $y = \{c, b\}$, c and b represent categories and bounding boxes, respectively. Similar to RT-DETR, we incorporate the IoU score into the objective function of the classification branch, following the approach from VFL [44], to enforce consistency between the classification and localization of positive samples. \mathcal{L}_{box} includes the L1 loss and the generalized IoU loss [25], which are not described here. And, the auxiliary loss from DAB-DETR [15] is also employed in our approach.

The second objective addresses a metric learning problem, specifically the learning of an embedding space where instances of the same identity are close to each other while those of different identities are far apart. Previous methods like JDE [35] and FairMOT [45] used one-hot labels. While this approach is simple and effective, it requires prior knowledge of the number of IDs in the training set to configure the output dimensions of the ID embedding head. This requirement obviously limits the model’s generalization capability and becomes impractical in dense scenarios, as it leads to excessively high embedding dimensions. Moreover, subsequent Transformer-based tracking models predominantly rely on queries for tracking, and the drawbacks of this method have been discussed earlier.

MOTIP [11] employs a predefined ID dictionary and classification methods for object association, whereas PuTR utilizes an association method based on embedding similarity. These two approaches are undoubtedly more generalizable. However, possibly because their decoders primarily process the trajectories of object movements when outputting embeddings, and since the queries used by FastTrackTr to generate embeddings contain more image features and positional information of the current target, these methods fail to enable FastTrackTr to achieve satisfactory convergence.

To address the aforementioned issues, we need to find a method more suitable for image features and with greater generalizability for generating ID embeddings. Therefore, we turn our attention to the training methods of ReID (Re-identification) models. By converting the generation of ID embeddings into a ReID problem, we only need to consider the distances and similarities between embeddings, thereby enhancing the model’s generalization capability.

For the above reasons and for better performance, in this paper, we adopt the more advanced circle loss [33] in this

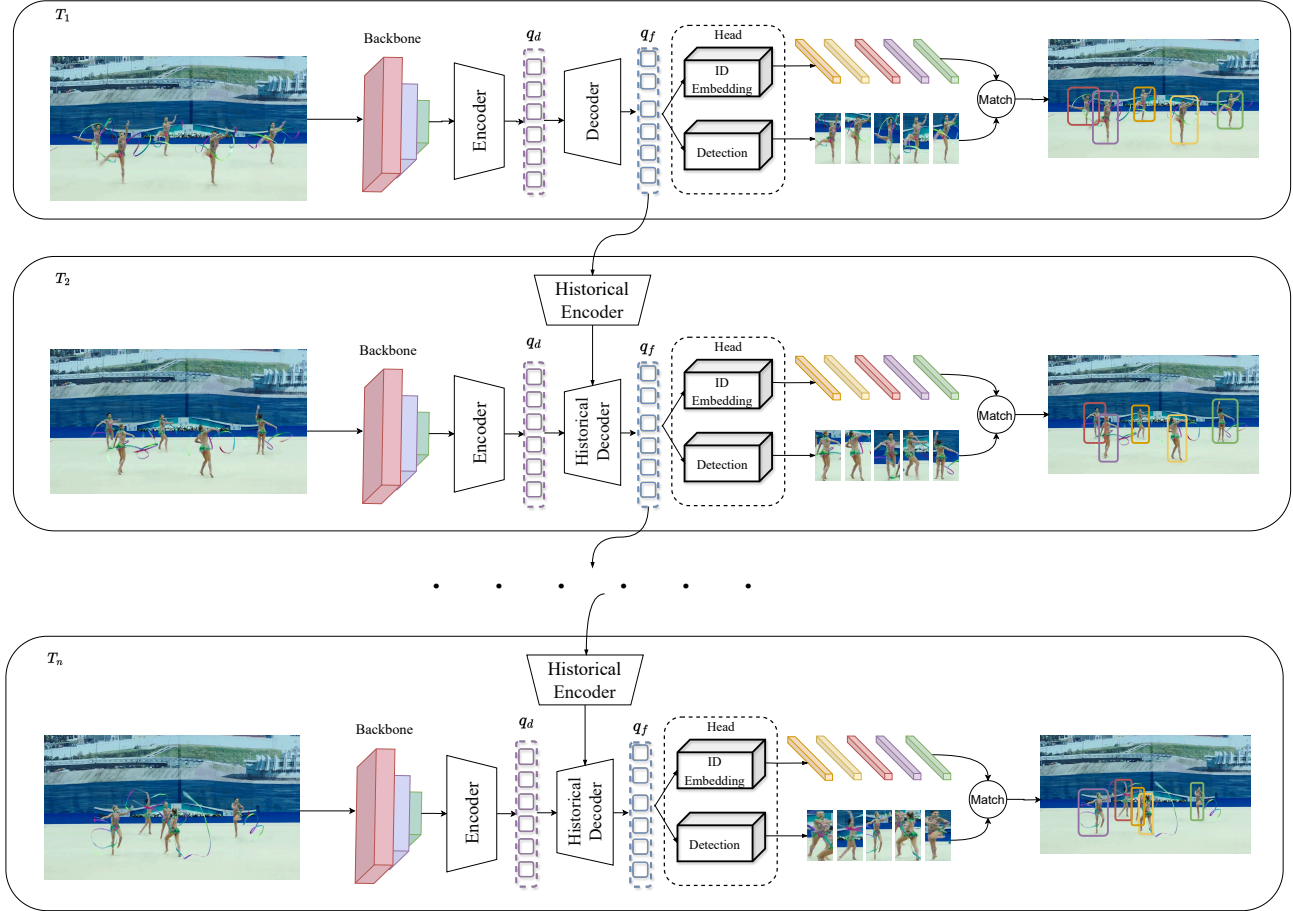


Figure 2. The complete structure of FastTrackTr. For the initial frame, the model functions as a detection system, assigning unique identifiers to each detected object. Subsequently, from the second frame onwards, the historical queries from previous frames and their corresponding masks undergo processing through a single-layer encoder. The output and image feature of this frame are then fed into a historical-cross decoder. Based on the head’s output, detection results and ID embeddings are generated. These are then matched and associated with previous results to produce the final tracking outcome. This architecture achieves the efficient tracking, which can be run in real time on some devices.

work. Specifically, the id embeddings of the same object between multiple frames is treated as positive pairs denoted as s_p and between different objects as negative samples denoted as s_n , respectively. $-\alpha_p$ and α_n are the adaptive weighting factors for positive and negative samples, determined by the following equations:

$$\alpha_p = [O_p - s_p]^+, \quad \alpha_n = [s_n - O_n]^+ \quad (2)$$

where $O_p = 1 + m$ and $O_n = -m$, with m being a margin hyperparameter. These terms adjust the weight of each sample based on its distance from the ideal similarity value. The margins $\Delta_p = 1 - m$ and $\Delta_n = m$ are used to further separate positive and negative pairs in the embedding space.

The logits for positive and negative pairs are then computed as:

$$\log_p = -\gamma\alpha_p(s_p - \Delta_p), \quad \log_n = \gamma\alpha_n(s_n - \Delta_n) \quad (3)$$

Finally, the unified Circle Loss function is formulated as follows:

$$\mathcal{L}_{\text{reid}} = \log \left[1 + \sum_{j=1}^L \exp(\gamma(\alpha_n^j (s_n^j - \Delta_n))) \sum_{i=1}^K \exp(-\gamma(\alpha_p^i (s_p^i - \Delta_p))) \right] \quad (4)$$

This formulation allows for a dynamic weighting of positive and negative pairs, enhancing the model’s ability to discriminate between similar and dissimilar identities. Circle Loss has proven to be an effective solution for embed-

ding learning in tasks that require fine-grained discrimination, which aligns with the goals of appearance embedding in our tracking framework.

The final total loss is as follows:

$$\mathcal{L}_{overall} = \lambda_{reid} * \mathcal{L}_{reid} + \lambda_{det} * \mathcal{L}_{det} \quad (5)$$

where λ_{reid} and λ_{det} are proportional coefficients used to balance the loss. In this paper, both of them are set to 1. Notably, it should be noted that, when computing the ReID loss, similar to the detection loss, the outputs from each decoder layer are incorporated into the calculation.

3.3. Historical Decoder and Encoder

Historical Decoder: Previous DETR-based MOT models[10, 20, 43] typically feed the final output queries of the previous frame, after some processing, directly into the decoder of the current frame to achieve tracking. This is an explicit tracking method, but it increases the number of queries, thereby increasing computational costs. To more efficiently utilize these historical queries, we replaced the self-attention mechanism in DETR’s decoder with a cross-attention mechanism to process the query features between consecutive frames. This significantly reduces the computational load. The differences between our decoder and the standard decoder are shown in Figure 3.

Specifically, each decoder module in DETR [4] consists of a sequential structure comprising a self-attention layer for the queries, a visual cross-attention layer, and a feed-forward neural network (FFN). Initially, the self-attention layer performs global modeling over the queries to enhance the model’s object detection performance. To further leverage historical information and improve tracking accuracy, we concatenate the final decoder output from frame $t - 1$, denoted as q_f^{t-1} , which is processed by the trajectory encoder, with the initial queries q_d^t of frame t . This concatenation replaces the key and value in the self-attention layer while keeping the queries unchanged. The implementation can be formally expressed as follows:

$$Q_T = \text{Linear}(q_d^t), \quad K_T = V_T = \text{Linear}(\text{concat}(q_d^t, q_f^{t-1})) \quad (6)$$

where $Q_T \in \mathbb{R}^{N \times C}$, K_T and $V_T \in \mathbb{R}^{2N \times C}$. Then, we calculate the query-trajectory attention map $A_T \in \mathbb{R}^{2N \times N}$, and aggregate informative depth features weighted by A_T to produce the Historical-aware queries q' , formulated as:

$$A_T = \text{Softmax}\left(\frac{Q_T K_T}{\sqrt{C}}\right) \quad (7)$$

$$q' = \text{Linear}(A_T V_T)$$

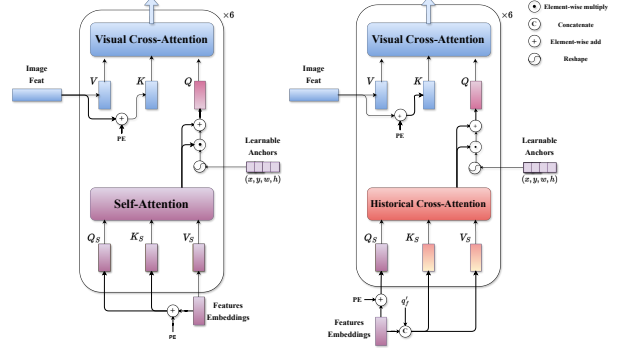


Figure 3. Schematic of the flow of our historical-cross decoder and a general decoder. Compared to a general decoder, ours replaces self-attention with historical cross-attention.

This mechanism allows each object query to adaptively capture features of the same object from images across consecutive frames, thereby achieving better object understanding. The queries with estimated historical information are then input into the inter-query self-attention layer for feature interaction between objects, and the visual cross-attention layer for collecting visual semantics. We use 6 decoder layers.

Historical Encoder: In FastTrackTr, we have introduced an additional Historical Encoder to enhance the modeling of temporal relationships, and we utilize a masking mechanism during the self-attention process to provide contextual priors for the tracked objects. For the historical feature information from the previous frame or multiple frames, only a subset of the data is utilized. To effectively model these historical data, we employ a masking mechanism and process the data through standard encoder layers. During training, the generation of masks is determined by the ground truth labels, while in inference, masks are based on confidence scores to decide which objects to retain.

The workflow of the historical encoder is illustrated in Figure 4. After generating the mask, we fuse the decoder output q_f^t with the historical information q_f^{t-1} through an attention mechanism, computed as follows:

$$Q_E = K_E = \text{Linear}\left(q_f^{t-1} + q_{pos}\right), V_E = \text{Linear}(q_f^t) \quad (8)$$

The attention calculation follows the same formula as previously used in the decoder, which is not repeated here. Finally, the fused features are processed by an additional network layer to obtain q_f^t . It is noted that for $t = 1$, $q_f^{t-1} = q_f^t$.

The mask generation module in this method includes two modes: (1) In the training phase, the mask is determined by ground truth information, generated by checking if each

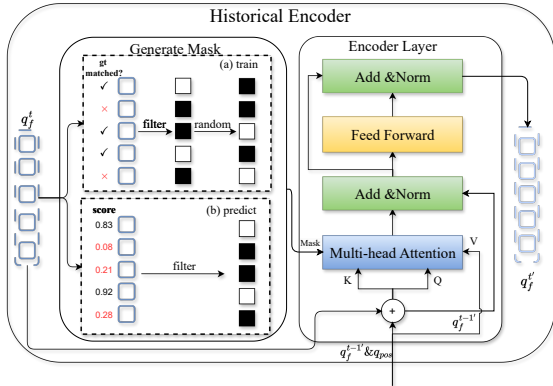


Figure 4. Schematic of the flow of our Historical Encoder. The main role of this Encoder is to further aggregate the temporal features. The generated mask is randomly inverted partially during training. The probability of reversal is related to the number of truth values.

object matches with the ground truth labels, and random sampling of the masks is performed to flip them, enhancing the model’s robustness; (2) In the inference phase, the mask is determined based on the confidence score of each object, with objects below a certain threshold being filtered out, while high-confidence objects are retained. This masking mechanism ensures that the model focuses on processing significant historical information, thereby improving the encoder’s capability to model the temporal dynamics of target trajectories.

3.4. Matching and Association

Although matching and association and not the primary focus of our paper, it is essential to outline some details of this process. Following the work of JDE, for a given video, after processing each frame, the model outputs detection results along with their corresponding ID embeddings. We then use these values to compute a similarity matrix between the embeddings of the observations and those of the existing tracking chains. The Hungarian algorithm is employed to assign observations to tracking chains. Subsequently, a Kalman filter is used to smooth the trajectories and predict the position of the previous frame’s tracking chain in the current frame. If the assigned observations are spatially distant from the predicted position, the assignment is rejected. Finally, the embeddings of the tracking chains are updated as follows:

$$f_t = \eta f_{t-1} + (1 - \eta) \tilde{f} \quad (9)$$

where \tilde{f} indicates the embedding of the assigned observation, and f_t indicates the embedding of the tracklet at

frame t , η is a momentum term for smoothing, and we set $\eta = 0.9$.

Of course, considering that there are now many optimized methods for this process, we have also implemented several validated, simple, and effective techniques to enhance this workflow. Specific improvements and their impacts can be found in the appendix.

4. Experiments

4.1. Setting

Datasets: Our proposed method mainly evaluated on DanceTrack [32] and SportsMOT [6], two recently introduced datasets with large-scale training data, which helps prevent overfitting. Both datasets also provide official validation sets, allowing for exploratory experiments. Additionally, we present results on the MOT17 [21] benchmark.

Metrics: We assessed our method using widely recognized MOT evaluation metrics. The primary metrics employed for evaluation included HOTA, AssA, DetA, IDF1 and MOTA [18, 26]. These metrics collectively provided a comprehensive and robust evaluation of our method’s tracking performance.

Implementation Details: For inference speed, our FastTrackTr is built on RT-DETR [48], with ResNet50 [13] as the backbone unless specified otherwise. The model is implemented in PyTorch [23], and the training is conducted on 8 NVIDIA RTX 4090 GPUs. The sequence length for training is set to 8 unless otherwise noted.

All ablation experiments use an image size of 640×640 . For further testing of the best tracking accuracy of our method, we use an image size of 800×1333 when comparing with SOTA methods. The Trajectory Encoder during training applies random mask transformations, with the probability related to the number of ground-truth objects. Given the number of ground-truth objects n_{gt} and the number of queries n_q , the probability of a non-masked flip is $\min(0.5, 2 \cdot n_{gt}/n_q)$, while for the rest, the probability is $\min(\max(0.1, n_{gt}/n_q), 0.2)$. For all three datasets, n_q is set to 300. Dancetrack and SportMOT are trained for 27 epochs, while MOT17 is trained for 80 epochs. The optimizer is AdwM [17] with a learning rate of 10^{-4} and weight decay of 5.0×10^{-4} . Due to GPU memory limitations, the batch size is set to 4 for smaller images and 1 for larger images. Lastly, for all datasets, the final output dimension of ID embedding is 256.

4.2. Main Result

Comprehensive Comparison of Speed and Accuracy: Table 1 highlights FastTrackTr’s superior latency performance compared to existing methods on the Dancetrack validation set. FastTrackTr consistently delivers faster processing speeds while maintaining competitive HOTA scores,

Table 1. Overall Latency comparison between FastTrackTr and existing methods on the Dancetrack [32] val. Methods highlighted in gray utilize the YOLOX [12] detector, with its processing time included. Similarly, the latency of our method accounts for its associated time consumption, demonstrating efficient performance with the chosen configuration. Dec³ refers to a 3-layer decoder layer, while R18 refers to ResNet18.

Methods	Image Res.	Numerical Precision	Overall Latency(ms)	HOTA
DeepOC-SORT[19]	1440 × 800	FP16	28.1ms (35.6fps)	58.5
SUSHI[5]	1440 × 800	FP32/FP16	42.9ms (23.3fps) / 38.6ms (25.9fps)	/
PuTR[14]	1440 × 800	FP32/FP16	30.5ms (32.8fps) / 28.2ms (35.5fps)	55.7
MOTR [43]	1333 × 800	FP32/FP16	60.0ms (16.5fps) / 52.9ms (18.9fps)	51.3
MOTIP[11]	1333 × 800	FP32/FP16	61.7ms (16.2fps) / 45.7ms (21.8fps)	59.1
FastTrackTr	1333 × 800	FP32/FP16	40.2ms (24.8fps) / 30.9ms (32.4fps)	56.8
MOTIP(RT-DETR)	640 × 640	FP32/FP16	32.1ms (31.2fps) / 24.5ms (40.8fps)	56.2
FastTrackTr	640 × 640	FP32/FP16	23.6ms (42.3fps) / 19.6ms (51.0fps)	54.1
FastTrackTr-Dec ³	640 × 640	FP32/FP16	20.4ms (49.0fps) / 14.8ms (67.6fps)	51.2
FastTrackTr-R18-Dec ³	640 × 640	FP32/FP16	12.8ms (78.0fps) / 9.86ms (101.4fps)	47.4

Table 2. Performance comparison between FastTrackTr and existing methods on the Dancetrack [32] test set. The best performance among the methods is marked in **bold** and please pay more attention to the metrics with *.

Methods	HOTA*	DetA	AssA	MOTA	IDF1
FairMOT[45]	39.7	66.7	23.8	82.2	40.8
CenterTrack [49]	41.8	78.1	22.6	86.8	35.7
TraDeS [37]	43.3	74.5	25.4	86.2	41.2
TransTrack[31]	45.5	75.9	27.5	88.4	45.2
ByteTrack [46]	47.7	71.0	32.1	89.6	53.9
GTR[50]	48.0	72.5	31.9	84.7	50.3
QDTrack[9]	54.2	80.1	36.8	87.7	50.4
MOTR [43]	54.2	73.5	40.2	79.7	51.5
OC-SORT [3]	55.1	80.3	38.3	92.0	54.6
PuTR[14]	55.8	/	/	91.9	58.2
C-BIoU [40]	60.6	81.3	45.4	91.6	61.6
CMTrack [29]	61.8	/	46.4	92.5	63.3
FastTrackTr(ours)	62.4	78.4	49.8	88.8	64.8

demonstrating efficient real-time capabilities. Additionally, its performance scales effectively with reduced image resolutions, further enhancing its applicability. Advanced variants of FastTrackTr achieve even higher frame rates with only minimal compromises in tracking accuracy. These advantages make FastTrackTr highly effective for practical multi-object tracking applications.

Comparison of State-Of-The-Art: To better demonstrate the superiority of our FastTrackTr, we employed nearly all available data augmentations and used larger image sizes. Tables 2, 3, and 4 respectively showcase the maximum tracking performance of FastTrackTr on DanceTrack, SportsMOT, and MOT17 benchmark. Similar to many previous works [10, 43, 47, 49], we utilized the CrowdHuman [28] dataset for data augmentation on MOT17 and DanceTrack. It is important to note that although our method still does not outperform CNN-based models on the MOT17 benchmark, the underlying reason remains the

Table 3. Performance comparison with state-of-the-art methods on SportsMOT [6].

Methods	HOTA*	DetA	AssA	MOTA	IDF1
FairMOT [45]	49.3	70.2	34.7	86.4	53.5
QDTrack [9]	60.4	77.5	47.2	90.1	62.3
ByteTrack [46]	62.1	76.5	50.5	93.4	69.1
OC-SORT [3]	68.1	84.8	54.8	93.4	68.0
MeMOTR [10]	68.8	82.0	57.8	90.2	69.9
FastTrackTr(ours)	70.1	83.9	58.6	94.0	72.0

well-discussed issue: for transformer models, the amount of data in the MOT17 dataset is too limited. Nevertheless, our method has surpassed all previous transformer-based approaches. This indicates that our method performs better even when the dataset images do not allow for sufficient training of the model, suggesting that our approach has potential for practical application in real-world settings, rather than being confined mostly to academic research like previous transformer methods, with few exceptions.

4.3. Ablation Study

We tested the impact of various components of our model and other factors on performance on the val set of **DanceTrack**.

The ablation study in Table 5 highlights the progressive enhancements of FastTrackTr on the DanceTrack validation set. Starting with a baseline HOTA of 47.3, adding the Decoder increases HOTA to 51.6, AssA to 37.2, and IDF1 to 51.3. Incorporating both Decoder and Encoder further boosts HOTA to 53.8, AssA to 39.9, and IDF1 to 53.5. Finally, including the Mask module achieves the highest scores with HOTA of 54.1, AssA of 40.0, and IDF1 of 54.7. These results demonstrate that each component significantly contributes to the overall tracking performance of FastTrackTr.

Table 4. Performance comparison with state-of-the-art methods on MOT17 [21]. The best performance among the transformer-based methods is marked in bold.

Methods	HOTA*	DetA	AssA	MOTA	IDF1
CNN based:					
CenterTrack [49]	52.2	53.8	51.0	67.8	64.7
QDTrack [9]	53.9	55.6	52.7	68.7	66.3
FairMOT [45]	59.3	60.9	58.0	73.7	72.3
ByteTrack [46]	63.1	64.5	62.0	80.3	77.3
OC-SORT [3]	63.2	63.2	63.4	78.0	77.5
C-BIoU [40]	64.1	64.8	63.7	81.1	79.7
MotionTrack [24]	65.1	65.4	65.1	81.1	80.1
Transformer based:					
TrackFormer [20]	/	/	/	74.1	68.0
TransTrack [31]	54.1	61.6	47.9	74.5	63.9
TransCenter [38]	54.5	60.1	49.7	73.2	62.2
MeMOT [2]	56.9	/	55.2	72.5	69.0
MOTR [43]	57.2	58.9	55.8	71.9	68.4
MOTIP [11]	59.2	62.0	56.9	75.5	71.2
PuTR[14]	61.1	/	/	74.8	74.1
FastTrackTr(our)	62.4	62.8	63.0	76.7	77.2

Table 5. Ablation Study of our proposed FastTrackTr on the DanceTrack validation set.

Decoder	Encoder	Mask	HOTA	AssA	IDF1
			47.3	32.5	46.3
✓			51.6	37.2	51.3
✓	✓		53.8	39.9	53.5
✓	✓	✓	54.1	40.0	54.7

Table 6. The Impact of Different Historical Cross Attention mechanisms on Tracking Performance

k	v	HOTA	DetA	AssA	IDF1
q^t	q_f^{t-1}	48.8	70.4	35.8	48.1
q_f^{t-1}	q_f^{t-1}	48.2	70.0	33.0	47.7
$q_f^{t-1'}$	q^t	49.0	71.5	35.9	48.5
concat	concat	51.6	72.8	37.2	51.3

In Table 6, we demonstrate the impact of different trajectory cross-attention mechanisms within the trajectory decoder on tracking performance. Here, q^t represents the original query, while q_f^{t-1} denotes the output of the decoder from the previous frame, with 'concat' indicating their concatenation. It is important to note that in this table, q_f^{t-1} has not passed through the trajectory encoder, hence its performance is not as good as that of the final model.

Table 7 analyzes the effect of different training frame counts on long-term fusion performance. Utilizing 8 frames yields the highest HOTA, demonstrating superior tracking accuracy. Compared to using fewer frames, 8 frames offer substantial performance improvements while maintaining efficient training times. Beyond 8 frames, metrics show minimal or negligible gains, indicating diminishing

Table 7. Training frames for long-term fusion.

Training frames	HOTA	DetA	AssA	IDF1
3	51.7	72.8	36.7	50.9
5	53.5	74.2	38.8	53.5
8	54.1	75.6	40.0	54.7
9	54.0	75.4	39.6	54.8
10	54.1	75.8	39.8	54.6

Table 8. The impact of various ID Embeddings losses on performance.

loss	HOTA	DetA	AssA	IDF1
triplet loss	52.7	76.8	38.1	52.4
one hot	53.8	75.2	39.4	54.1
circle loss	54.1	75.6	40.0	54.7

returns with additional frames. Thus, selecting 8 training frames provides an optimal balance between enhanced performance and training efficiency for FastTrackTr.

In Table 8, we demonstrate the impact of using circle loss [33], triplet loss [27], and one-hot encoding loss of the JDE [35] on our method performance during the training of ID embeddings. From the result, circle loss consistently outperforms both triplet loss and one-hot encoding loss across all metrics. Specifically, circle loss achieves the highest tracking performance. In comparison, triplet loss shows the lowest performance, and one-hot encoding loss provides intermediate results. These results demonstrate that circle loss effectively enhances the training of ID embeddings, leading to superior tracking performance in our method.

5. Conclusion and Limitations

Conclusion: In this paper, we introduce a rapid tracking method, FastTrackTr, which demonstrates superior performance across multiple datasets. By incorporating novel trajectory encoder and decoder designs, we effectively enhance the accuracy and robustness of tracking. Additionally, FastTrackTr achieves significant improvements in computational efficiency, presenting substantial potential for real-time applications. Future work will focus on further optimizing the model structure to adapt to more complex scenarios and exploring deployment possibilities across different hardware platforms.

Limitations: The primary limitation of FastTrackTr is its tracking accuracy, which does not surpass that of MOTIP. This issue likely arises because MOTIP employs a specialized network structure for ID encoding and its training method for long sequences, which ensures better temporal information learning. As the saying goes, "there are trade-offs"; these aspects also result in poor inference speed and slow training for MOTIP. Conversely, FastTrackTr does not exhibit these drawbacks.

References

- [1] Alex Bewley, Zongyuan Ge, Lionel Ott, Fabio Ramos, and Ben Upcroft. Simple online and realtime tracking. In *2016 IEEE International Conference on Image Processing (ICIP)*, pages 3464–3468, 2016. 1
- [2] Jiarui Cai, Mingze Xu, Wei Li, Yuanjun Xiong, Wei Xia, Zhuowen Tu, and Stefano Soatto. Memot: Multi-object tracking with memory. In *Proceedings of the IEEE/CVF Conference on Computer Vision and Pattern Recognition*, pages 8090–8100, 2022. 2, 8
- [3] Jinkun Cao, Jiangmiao Pang, Xinshuo Weng, Rawal Khirrodkar, and Kris Kitani. Observation-centric sort: Rethinking sort for robust multi-object tracking. In *Proceedings of the IEEE/CVF Conference on Computer Vision and Pattern Recognition*, pages 9686–9696, 2023. 2, 7, 8
- [4] Nicolas Carion, Francisco Massa, Gabriel Synnaeve, Nicolas Usunier, Alexander Kirillov, and Sergey Zagoruyko. End-to-end object detection with transformers. In *European conference on computer vision*, pages 213–229. Springer, 2020. 3, 5
- [5] Orcun Cetintas, Guillem Brasó, and Laura Leal-Taixé. Unifying short and long-term tracking with graph hierarchies. In *Proceedings of the IEEE/CVF Conference on Computer Vision and Pattern Recognition*, pages 22877–22887, 2023. 2, 7
- [6] Yutao Cui, Chenkai Zeng, Xiaoyu Zhao, Yichun Yang, Gangshan Wu, and Limin Wang. Sportsmot: A large multi-object tracking dataset in multiple sports scenes. In *Proceedings of the IEEE/CVF International Conference on Computer Vision*, pages 9921–9931, 2023. 2, 6, 7, 14
- [7] Yunhao Du, Zhicheng Zhao, Yang Song, Yanyun Zhao, Fei Su, Tao Gong, and Hongying Meng. StrongSORT: Make DeepSORT Great Again. *IEEE Transactions on Multimedia*, pages 1–14, 2023. 1
- [8] Christoph Feichtenhofer, Axel Pinz, and Andrew Zisserman. Detect to track and track to detect. In *Proceedings of the IEEE international conference on computer vision*, pages 3038–3046, 2017. 3
- [9] Tobias Fischer, Thomas E Huang, Jiangmiao Pang, Linlu Qiu, Haofeng Chen, Trevor Darrell, and Fisher Yu. Qdtrack: Quasi-dense similarity learning for appearance-only multiple object tracking. *IEEE Transactions on Pattern Analysis and Machine Intelligence*, 2023. 7, 8
- [10] Ruopeng Gao and Limin Wang. Memotr: Long-term memory-augmented transformer for multi-object tracking. In *Proceedings of the IEEE/CVF International Conference on Computer Vision*, pages 9901–9910, 2023. 1, 2, 5, 7
- [11] Ruopeng Gao, Yijun Zhang, and Limin Wang. Multiple object tracking as id prediction. *arXiv preprint arXiv:2403.16848*, 2024. 1, 2, 3, 7, 8
- [12] Z Ge. Yolox: Exceeding yolo series in 2021. *arXiv preprint arXiv:2107.08430*, 2021. 7
- [13] Kaiming He, Xiangyu Zhang, Shaoqing Ren, and Jian Sun. Deep residual learning for image recognition. In *Proceedings of the IEEE conference on computer vision and pattern recognition*, pages 770–778, 2016. 3, 6
- [14] Chongwei Liu, Haojie Li, Zhihui Wang, and Rui Xu. Putr: A pure transformer for decoupled and online multi-object tracking. *arXiv preprint arXiv:2405.14119*, 2024. 2, 7, 8
- [15] Shilong Liu, Feng Li, Hao Zhang, Xiao Yang, Xianbiao Qi, Hang Su, Jun Zhu, and Lei Zhang. Dab-detr: dynamic anchor boxes are better queries for detr. 2022. 3
- [16] Zelin Liu, Xinggang Wang, Cheng Wang, Wenyu Liu, and Xiang Bai. Sparsetrack: Multi-object tracking by performing scene decomposition based on pseudo-depth. *arXiv preprint arXiv:2306.05238*, 2023. 2
- [17] Ilya Loshchilov and Frank Hutter. Decoupled weight decay regularization. *arXiv preprint arXiv:1711.05101*, 2017. 6
- [18] Jonathon Luiten, Aljosa Osep, Patrick Dendorfer, Philip Torr, Andreas Geiger, Laura Leal-Taixé, and Bastian Leibe. Hota: A higher order metric for evaluating multi-object tracking. *International journal of computer vision*, 129:548–578, 2021. 6
- [19] Gerard Maggolino, Adnan Ahmad, Jinkun Cao, and Kris Kitani. Deep OC-SORT: Multi-Pedestrian Tracking by Adaptive Re-Identification, 2023. 1, 2, 7, 13
- [20] Tim Meinhardt, Alexander Kirillov, Laura Leal-Taixé, and Christoph Feichtenhofer. Trackformer: Multi-object tracking with transformers. In *Proceedings of the IEEE/CVF conference on computer vision and pattern recognition*, pages 8844–8854, 2022. 1, 2, 5, 8
- [21] Anton Milan, Laura Leal-Taixé, Ian Reid, Stefan Roth, and Konrad Schindler. MOT16: A Benchmark for Multi-Object Tracking, 2016. 2, 6, 8, 14
- [22] Liao Pan, Yang Feng, Wu Di, Liu Bo, and Zhang Xingle. Mo-yolo: End-to-end multiple-object tracking method with yolo and motr. *arXiv preprint arXiv:2310.17170*, 2023. 1
- [23] Adam Paszke, Sam Gross, Francisco Massa, Adam Lerer, James Bradbury, Gregory Chanan, Trevor Killeen, Zeming Lin, Natalia Gimelshein, Luca Antiga, et al. Pytorch: An imperative style, high-performance deep learning library. *Advances in neural information processing systems*, 32, 2019. 6
- [24] Zheng Qin, Sanping Zhou, Le Wang, Jinghai Duan, Gang Hua, and Wei Tang. Motiontrack: Learning robust short-term and long-term motions for multi-object tracking. In *Proceedings of the IEEE/CVF conference on computer vision and pattern recognition*, pages 17939–17948, 2023. 2, 8
- [25] Hamid Rezaatofighi, Nathan Tsoi, JunYoung Gwak, Amir Sadeghian, Ian Reid, and Silvio Savarese. Generalized intersection over union: A metric and a loss for bounding box regression. In *Proceedings of the IEEE/CVF conference on computer vision and pattern recognition*, pages 658–666, 2019. 3
- [26] Ergys Ristani, Francesco Solera, Roger Zou, Rita Cucchiara, and Carlo Tomasi. Performance measures and a data set for multi-target, multi-camera tracking. In *European conference on computer vision*, pages 17–35. Springer, 2016. 6
- [27] Florian Schroff, Dmitry Kalenichenko, and James Philbin. Facenet: A unified embedding for face recognition and clustering. In *Proceedings of the IEEE conference on computer vision and pattern recognition*, pages 815–823, 2015. 8

- [28] Shuai Shao, Zijian Zhao, Boxun Li, Tete Xiao, Gang Yu, Xiangyu Zhang, and Jian Sun. Crowdhuman: A benchmark for detecting human in a crowd. *arXiv preprint arXiv:1805.00123*, 2018. 7
- [29] Kyujin Shim, Jubi Hwang, Kangwook Ko, and Changick Kim. A confidence-aware matching strategy for generalized multi-object tracking. In *2024 IEEE International Conference on Image Processing (ICIP)*, pages 4042–4048. IEEE, 2024. 7
- [30] Vivek Hari Sridhar, Dominique G Roche, and Simon Giggins. Tracktor: image-based automated tracking of animal movement and behaviour. *Methods in Ecology and Evolution*, 10(6):815–820, 2019. 3
- [31] Peize Sun, Jinkun Cao, Yi Jiang, Rufeng Zhang, Enze Xie, Zehuan Yuan, Changhu Wang, and Ping Luo. Transtrack: Multiple object tracking with transformer. *arXiv preprint arXiv:2012.15460*, 2020. 1, 2, 7, 8
- [32] Peize Sun, Jinkun Cao, Yi Jiang, Zehuan Yuan, Song Bai, Kris Kitani, and Ping Luo. DanceTrack: Multi-Object Tracking in Uniform Appearance and Diverse Motion. In *2022 IEEE/CVF Conference on Computer Vision and Pattern Recognition (CVPR)*, pages 20961–20970, New Orleans, LA, USA, 2022. IEEE. 2, 6, 7, 13
- [33] Yifan Sun, Changmao Cheng, Yuhan Zhang, Chi Zhang, Liang Zheng, Zhongdao Wang, and Yichen Wei. Circle loss: A unified perspective of pair similarity optimization. In *Proceedings of the IEEE/CVF conference on computer vision and pattern recognition*, pages 6398–6407, 2020. 3, 8
- [34] Ashish Vaswani, Noam Shazeer, Niki Parmar, Jakob Uszkoreit, Llion Jones, Aidan N Gomez, Łukasz Kaiser, and Illia Polosukhin. Attention is all you need. *Advances in neural information processing systems*, 30, 2017. 1
- [35] Zhongdao Wang, Liang Zheng, Yixuan Liu, Yali Li, and Shengjin Wang. Towards real-time multi-object tracking. In *European conference on computer vision*, pages 107–122. Springer, 2020. 2, 3, 8, 12, 13
- [36] Nicolai Wojke, Alex Bewley, and Dietrich Paulus. Simple online and realtime tracking with a deep association metric. In *2017 IEEE international conference on image processing (ICIP)*, pages 3645–3649. IEEE, 2017. 2
- [37] Jialian Wu, Jiale Cao, Liangchen Song, Yu Wang, Ming Yang, and Junsong Yuan. Track to detect and segment: An online multi-object tracker. In *Proceedings of the IEEE/CVF conference on computer vision and pattern recognition*, pages 12352–12361, 2021. 7
- [38] Yihong Xu, Yutong Ban, Guillaume Delorme, Chuang Gan, Daniela Rus, and Xavier Alameda-Pineda. Transcenter: Transformers with dense representations for multiple-object tracking. *IEEE transactions on pattern analysis and machine intelligence*, 45(6):7820–7835, 2022. 2, 8
- [39] Feng Yan, Weixin Luo, Yujie Zhong, Yiyang Gan, and Lin Ma. Bridging the Gap Between End-to-end and Non-End-to-end Multi-Object Tracking. 1, 2
- [40] Fan Yang, Shigeyuki Odashima, Shoichi Masui, and Shan Jiang. Hard to track objects with irregular motions and similar appearances? make it easier by buffering the matching space. In *Proceedings of the IEEE/CVF winter conference on applications of computer vision*, pages 4799–4808, 2023. 7, 8
- [41] Mingzhan Yang, Guangxin Han, Bin Yan, Wenhua Zhang, Jinqing Qi, Huchuan Lu, and Dong Wang. Hybrid-sort: Weak cues matter for online multi-object tracking. In *Proceedings of the AAAI Conference on Artificial Intelligence*, pages 6504–6512, 2024. 1, 2, 13
- [42] En Yu, Tiancai Wang, Zhuoling Li, Yuang Zhang, Xiangyu Zhang, and Wenbing Tao. Motrv3: Release-fetch supervision for end-to-end multi-object tracking. *arXiv preprint arXiv:2305.14298*, 2023. 1, 2
- [43] Fangao Zeng, Bin Dong, Yuang Zhang, Tiancai Wang, Xiangyu Zhang, and Yichen Wei. Motr: End-to-end multiple-object tracking with transformer. In *European Conference on Computer Vision*, pages 659–675. Springer, 2022. 1, 2, 5, 7, 8
- [44] Haoyang Zhang, Ying Wang, Feras Dayoub, and Niko Sunderhauf. Varifocalnet: An iou-aware dense object detector. In *Proceedings of the IEEE/CVF conference on computer vision and pattern recognition*, pages 8514–8523, 2021. 3
- [45] Yifu Zhang, Chunyu Wang, Xinggang Wang, Wenjun Zeng, and Wenyu Liu. Fairmot: On the fairness of detection and re-identification in multiple object tracking. *International journal of computer vision*, 129:3069–3087, 2021. 2, 3, 7, 8
- [46] Yifu Zhang, Peize Sun, Yi Jiang, Dongdong Yu, Fucheng Wang, Zehuan Yuan, Ping Luo, Wenyu Liu, and Xinggang Wang. ByteTrack: Multi-object Tracking by Associating Every Detection Box. In *Computer Vision – ECCV 2022*, pages 1–21, Cham, 2022. Springer Nature Switzerland. 2, 7, 8, 13
- [47] Yuang Zhang, Tiancai Wang, and Xiangyu Zhang. Motrv2: Bootstrapping end-to-end multi-object tracking by pre-trained object detectors. In *Proceedings of the IEEE/CVF Conference on Computer Vision and Pattern Recognition*, pages 22056–22065, 2023. 2, 7
- [48] Yian Zhao, Wenyu Lv, Shangliang Xu, Jinman Wei, Guanzhong Wang, Qingqing Dang, Yi Liu, and Jie Chen. Detsr beat yolos on real-time object detection. In *Proceedings of the IEEE/CVF Conference on Computer Vision and Pattern Recognition*, pages 16965–16974, 2024. 2, 3, 6
- [49] Xingyi Zhou, Vladlen Koltun, and Philipp Krähenbühl. Tracking objects as points. In *European conference on computer vision*, pages 474–490. Springer, 2020. 3, 7, 8
- [50] Xingyi Zhou, Tianwei Yin, Vladlen Koltun, and Philipp Krähenbühl. Global tracking transformers. In *Proceedings of the IEEE/CVF Conference on Computer Vision and Pattern Recognition*, pages 8771–8780, 2022. 7
- [51] Xizhou Zhu, Weijie Su, Lewei Lu, Bin Li, Xiaogang Wang, and Jifeng Dai. Deformable detr: Deformable transformers for end-to-end object detection. *arXiv preprint arXiv:2010.04159*, 2020. 2
- [52] Zhenhua Zhu, Xiaoning Ren, and Zhi Chen. Integrated detection and tracking of workforce and equipment from construction jobsite videos. *Automation in Construction*, 81: 161–171, 2017. 3

A. More discussion on FastTrackTr

A.1. Description of calculations

In this section, we analyze the computational complexity of FastTrackTr and MOTR. The goal is to determine the threshold at which the computational cost of the MOTR exceeds that of our FastTrackTr when the number of queries increases. We focus on the decoder layer, including the self-attention, cross-attention, feed-forward network (FFN), and normalization layers.

A.1.1. Model Definitions

MOTR (Variable Query Number): The number of queries increases from N to $N_q = N + \Delta N$, where ΔN is the additional number of queries. Both the self-attention and subsequent components are affected by this increase.

FastTrackTr (Modified Self-Attention): The self-attention mechanism is altered such that the key and value tensors have dimensions $2N \times C$, while the query tensor remains $N \times C$. Other components retain their original computational complexity.

A.1.2. Notations

- N : Original number of queries.
- ΔN : Additional queries in MOTR ($N_q = N + \Delta N$).
- C : Dimensionality of each query.
- M : Length of the memory (number of keys/values in cross-attention).
- d_{ff} : Dimensionality of the FFN's hidden layer (typically $4C$).

A.1.3. Computational Complexity Analysis

MOTR:

1. Self-Attention:

$$\mathcal{O}_{\text{SA}_1} = (N + \Delta N)^2 \cdot C \quad (10)$$

2. Cross-Attention:

$$\mathcal{O}_{\text{CA}_1} = (N + \Delta N) \cdot M \cdot C \quad (11)$$

3. Feed-Forward Network (FFN):

$$\mathcal{O}_{\text{FFN}_1} = 2(N + \Delta N) \cdot C \cdot d_{\text{ff}} \quad (12)$$

(Two linear layers with activation in between.)

4. Layer Normalization:

$$\mathcal{O}_{\text{LN}_1} = 2(N + \Delta N) \cdot C \quad (13)$$

(Two LayerNorm layers.)

Total Complexity of MOTR:

$$\mathcal{O}_1 = (N + \Delta N)^2 \cdot C + (N + \Delta N) \cdot M \cdot C + 2(N + \Delta N) \cdot C \cdot d_{\text{ff}} + 2(N + \Delta N) \cdot C \quad (14)$$

FastTrackTr:

1. Self-Attention:

$$\mathcal{O}_{\text{SA}_2} = N \cdot (2N) \cdot C = 2N^2 \cdot C \quad (15)$$

2. Cross-Attention:

$$\mathcal{O}_{\text{CA}_2} = N \cdot M \cdot C \quad (16)$$

3. Feed-Forward Network (FFN):

$$\mathcal{O}_{\text{FFN}_2} = 2N \cdot C \cdot d_{\text{ff}} \quad (17)$$

4. Layer Normalization:

$$\mathcal{O}_{\text{LN}_2} = 2N \cdot C \quad (18)$$

Total Complexity of FastTrackTr:

$$\mathcal{O}_2 = 2N^2 \cdot C + N \cdot M \cdot C + 2N \cdot C \cdot d_{\text{ff}} + 2N \cdot C \quad (19)$$

A.1.4. Inequality for Computational Cost Comparison

To find the threshold ΔN where $\mathcal{O}_1 > \mathcal{O}_2$, we set up the inequality:

$$\begin{aligned} & (N + \Delta N)^2 \cdot C + (N + \Delta N) \cdot M \cdot C \\ & + 2(N + \Delta N) \cdot C \cdot d_{\text{ff}} + 2(N + \Delta N) \cdot C \\ & > 2N^2 \cdot C + N \cdot M \cdot C + 2N \cdot C \cdot d_{\text{ff}} + 2N \cdot C \end{aligned} \quad (20)$$

Simplifying the inequality by eliminating common terms and dividing both sides by C :

$$\begin{aligned} & (N + \Delta N)^2 - 2N^2 + (N + \Delta N - N) \cdot M \\ & + 2(N + \Delta N - N) \cdot d_{\text{ff}} + 2(N + \Delta N - N) > 0 \\ \Rightarrow & (N + \Delta N)^2 - 2N^2 + \Delta N \cdot (M + 2d_{\text{ff}} + 2) > 0 \end{aligned} \quad (21)$$

Expanding the square term:

$$\begin{aligned} & N^2 + 2N\Delta N + (\Delta N)^2 - 2N^2 \\ & + \Delta N \cdot (M + 2d_{\text{ff}} + 2) > 0 \end{aligned} \quad (22)$$

Combining like terms:

$$\begin{aligned} & -N^2 + 2N\Delta N + (\Delta N)^2 \\ & + \Delta N \cdot (M + 2d_{\text{ff}} + 2) > 0 \end{aligned} \quad (23)$$

Simplifying:

$$-N^2 + \Delta N (2N + \Delta N + M + 2d_{\text{ff}} + 2) > 0 \quad (24)$$

A.1.5. Determining the Threshold ΔN

To find the minimum ΔN satisfying the inequality, we proceed as follows.

$$-N^2 + \Delta N (2N + \Delta N + M + 2d_{\text{ff}} + 2) > 0 \quad (25)$$

A.1.6. Final Solution with Specific Numerical Values

Assuming typical values for a Deformable DETR decoder layer:

- Number of original queries: $N = 300$
- Memory length: $M = 8400$
- Query dimensionality: $C = 256$
- FFN hidden dimension: $d_{ff} = 4C = 1024$

Substituting the numerical values:

$$-(300)^2 + \Delta N \left(2 \times 300 + \Delta N + 8400 + 2 \times 1024 + 2 \right) > 0 \quad (26)$$

Computing constants:

$$-90,000 + \Delta N (600 + \Delta N + 8400 + 2048 + 2) > 0 \quad (27)$$

Simplifying the expression inside the parentheses:

$$-90,000 + \Delta N (\Delta N + 11,050) > 0 \quad (28)$$

Forming a quadratic inequality:

$$(\Delta N)^2 + 11,050\Delta N - 90,000 > 0 \quad (29)$$

Solving the quadratic equation:

$$(\Delta N)^2 + 11,050\Delta N - 90,000 = 0 \quad (30)$$

Using the quadratic formula:

$$\Delta N = \frac{-11,050 \pm \sqrt{(11,050)^2 - 4 \times 1 \times (-90,000)}}{2} \quad (31)$$

Calculating the discriminant:

$$D = (11,050)^2 + 360,000 = 122,102,500 + 360,000 = 122,462,500 \quad (32)$$

Finding the square root:

$$\sqrt{D} \approx 11,062.83 \quad (33)$$

Determining the positive root:

$$\Delta N = \frac{-11,050 + 11,062.83}{2} \approx \frac{12.83}{2} \approx 6.415 \quad (34)$$

The computational cost of MOTR exceeds that of FastTrackTr when the number of additional queries satisfies $\Delta N \geq 7$. This indicates that increasing the number of queries by at least seven will result in higher computational complexity for MOTR compared to FastTrackTr, considering all components of the decoder layer.

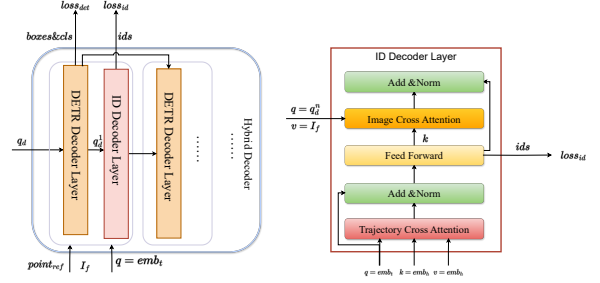


Figure 5. The proposed architecture features a hybrid decoder capable of facilitating end-to-end rapid tracking, which currently consists of six layers. There are two distinct types of layers within this decoder: the standard DETR layers, which are used to output detection results, and the ID decoder layers, which are dedicated to producing tracking outcomes. These layers are arranged alternately, with each type comprising three layers. This design aims to effectively merge detection and tracking functionalities within a single streamlined framework.

In summary, the computational load of FastTrackTr is generally lower than that of MOTR, except in scenarios where there are very few objects to track; in those cases, the theoretical computation may be slightly higher for FastTrackTr. Otherwise, FastTrackTr consistently requires less computational effort. Additionally, in practical applications, MOTR tends to be significantly slower due to memory constraints. For a detailed analysis, please refer to Section B.

A.2. Possibilities of End-to-end

We originally developed FastTrackTr with the goal of proposing a real-time, end-to-end multi-object tracking model. However, we observed that eliminating one decoder and directly applying MOTIP’s ID loss resulted in significant challenges in model convergence. Upon further analysis, we determined that although MOTIP’s ID loss appears similar to the appearance loss used in the previous JDT models, they fundamentally differ.

For models like JDE [35], the focus is on the similarity of object appearances, which does not incorporate specific object trajectories. In contrast, the ID decoder in MOTIP primarily handles trajectory information, with image data serving only as a supplementary element. The function and training method of this decoder might be similar to the entire PuTR model. Although our FastTrackTr attempts to integrate some temporal information by passing queries from one frame to the next, these queries predominantly contain image features. Under such conditions, supervising motion trajectories directly using MOTIP’s method becomes less effective, leading to poor or nearly impossible model convergence.

Following this analysis, we attempted to incorporate more historical information into the decoder. Our preliminary design introduces an identity-specific decoder layer into the traditional DETR architecture, as illustrated in Figure.5. These layers enhance alignment between current frame detections and corresponding identity features through a two-step attention mechanism, and link current detections with historical trajectories by emphasizing temporal consistency. The ID decoder layers are interlaced with standard DETR layers, initially comprising six layers in total.

The trajectory attention within the ID decoder layers can be formally described as follows:

$$\begin{aligned} Q_{ID} &= emb_t, & K_{ID} &= V_{ID} = emb_h \\ A_{ID} &= \text{Softmax} \left(\frac{Q_{ID}K_{ID}}{\sqrt{C}} \right) \\ q'_{ID} &= A_T V_T \end{aligned} \quad (35)$$

where emb_t and the input id decoder in MOTIP are the same. Its main components are the output of the previous decoder layer and the id encoding. emb_h is the historical encoding. Finally, the $q'_{ID} \in \mathbb{R}^{2 \times N \times C}$ will be reduced in dimension and fused through a conv layer and an FFN layer in the feedforward network.

The id loss used after the feedforward neural network and the id head is the id loss of MOTIP, which is shown below:

$$\begin{aligned} \mathcal{L}_{id} &= \frac{-\sum_{t=2}^{T+1} \sum_{m=1}^{M_t} \sum_{k=1}^{K+1} y_m^k \log(p_m^k)}{\sum_{t=2}^{T+1} M_t}, \\ y_m^k &= \begin{cases} 1 & \text{gt}_{id} \text{ of } m^{th} \text{ object is } k, \\ 0 & \text{else,} \end{cases} \end{aligned} \quad (36)$$

where $T + 1$ denotes the number of frames in a training clip, while there are M_t ground-truth objects in the t -th frame. y_m^k is an indicator function according to the identity ground truth of each object, as shown in Eq.(37). In practice, we simultaneously train object detector and ID predictor in an end-to-end strategy. Therefore, we leverage an overall loss function \mathcal{L} to supervise these two parts:

$$\mathcal{L} = \lambda_{det} \mathcal{L}_{det} + \lambda_{id} \mathcal{L}_{id} \quad (37)$$

Due to time constraints and the incomplete state of the model, we have conducted only one epoch of training on the DanceTrack dataset to observe whether the loss converges. After this single epoch, when employing the MOTIP process during inference, the HOTA score was approximately 16.7. This result preliminarily confirms that the model is broadly effective, with further fine-tuning required to optimize its performance.

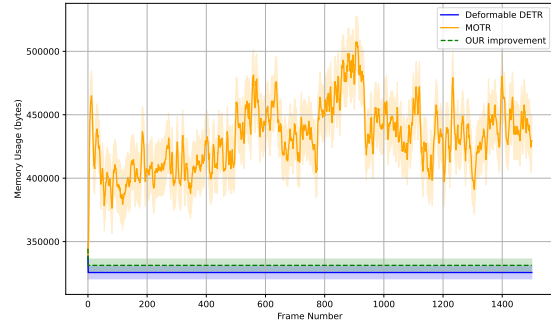


Figure 6. The changes in GPU memory consumption after the decoder for the MOTR, Deformable DETR, and our improved model in MOT17-03.

A.3. Improvements of the JDE association module

We believe that one of the reasons why JDT-type models have gradually been abandoned in recent years is that the commonly used JDE [35] association module has become somewhat outdated. This has led to JDT models underperforming compared to some of the more recent models. To better demonstrate the superiority of our approach, we made some minor adjustments to the JDE association method to improve its tracking performance.

Our improvements mainly focus on two aspects:

- 1) In the JDE association module, we associate only high-confidence detection boxes, ignoring those with lower confidence scores. By incorporating ByteTrack’s [46] bi-stage matching mechanism, we temporarily retain these low-confidence detection boxes as candidate targets. After matching the high-confidence targets, we perform a second round of matching using the high-confidence targets, which enhances tracking performance to some extent.
- 2) We also made some adjustments to the association strategy. In JDE, the first association is typically based on ID features, followed by a second association using historical trajectories. In our approach, similar to many other trackers, we include historical trajectories in the first round of association. Specifically, the cost matrix C is the weighted sum of the appearance cost A_a and the motion cost A_m , as follows:

$$C = \lambda A_a + (1 - \lambda) A_m \quad (38)$$

where the weight factor λ is set to 0.99, as in [19, 41].

A.4. More Implementation Details

By default, on DanceTrack [32], we train FastTrackTr for 27 epochs on the training set, dropping the learning rate by a

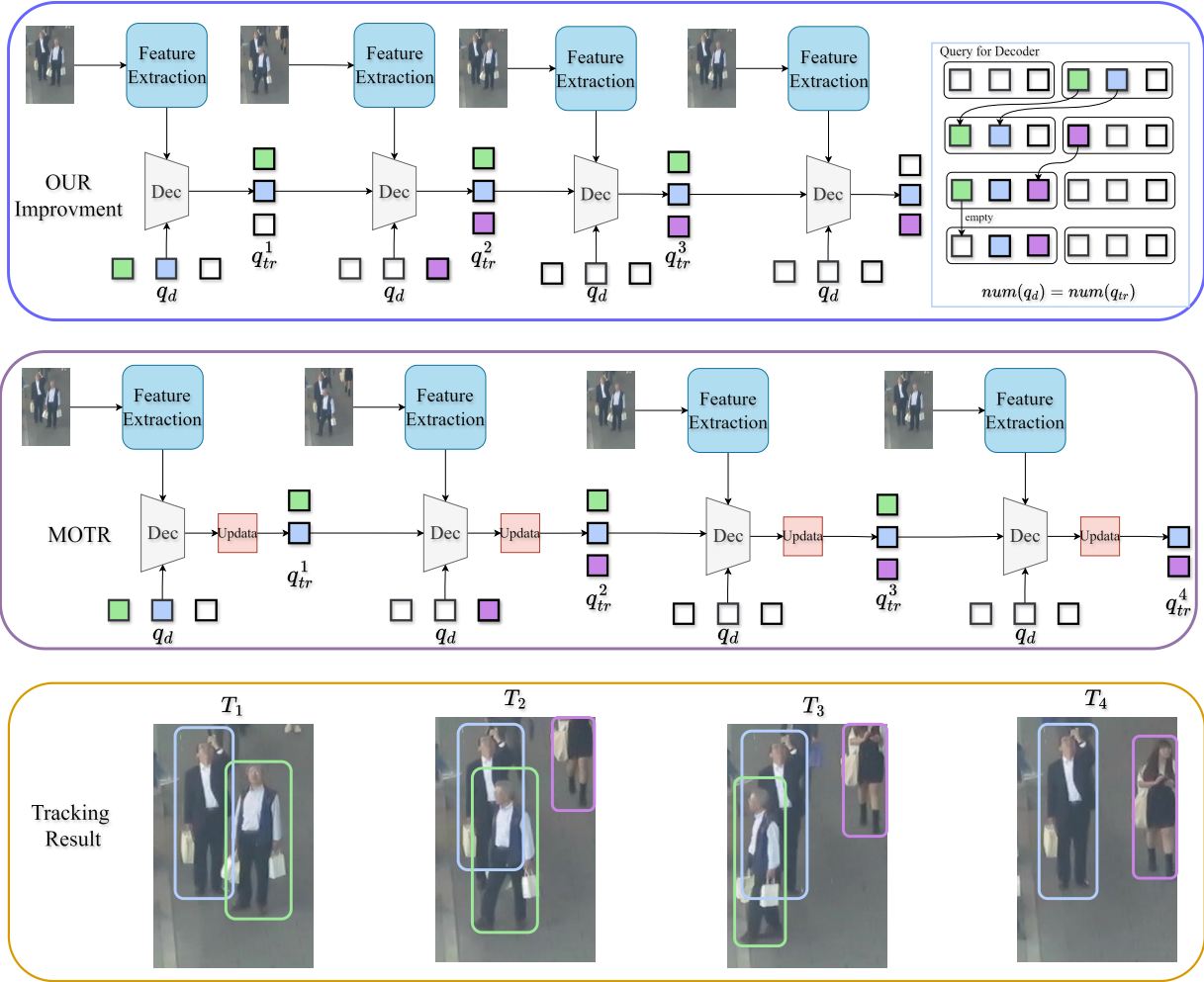


Figure 7. A simple MOTR and our improved tracking process diagram. The number of queries for MOTR will change, but after our improvement, it remains unchanged.

Table 9. Ablation Study of association module on the DanceTrack validation set.

Byte	Cost	HOTA	DetA	AssA	IDF1
		51.5	72.4	37.5	51.4
✓		53.4	74.3	39.7	53.1
	✓	52.4	73.1	38.3	52.6
✓	✓	54.1	75.6	40.0	54.7

factor of 10 at the 14th and 18th epochs. On SportsMOT [6], we train our model for 27 epochs on the training set, with the learning rate dropped at the 14th and 18th epochs. On MOT17 [21], we train the model on this combined training set for 80 epochs, with the learning rate dropped at the 45th and 55th epochs.

Table 10. Impact of different of positional encodings of the historical encode on the DanceTrack validation set.

Mechanism	HOTA	DetA	AssA	IDF1
w/o	53.8	74.9	39.5	53.8
MLP	53.5	74.2	38.9	53.5
decoder	54.1	75.6	40.0	54.7

For the additional use of the CrowdHuman dataset on DanceTrack and MOT17, our usage method follows the same approach as MOTIP. Interested readers can refer to the original work for further details.

Lastly, regarding the positional encoding of the historical encoder, the Table 10 shows the impact of different positional encodings on performance. In this table, "w/o" de-

notes the absence of positional encoding, "MLP" indicates that the positional encoding is generated from an MLP, and "decoder" refers to using the positional encoding from the final layer of the decoder.

B. How to Improve MOTR inference Speed

Although we have demonstrated in the previous sections that our FastTrackTr model generally requires less computation than the MOTR series of models, there remains an issue that puzzles us. Under the same configuration, models such as Deformable-DETR, MOTIP, and our FastTrackTr typically push GPU utilization to around 90%. However, MOTR only reaches about 40% on the same hardware (e.g., an RTX 4090), which is clearly problematic.

This led us to speculate whether the issue might be due to the dynamic nature of the query system, which could result in variable memory usage. As shown in Figure 6, we compare the memory consumption of the decoder when using fixed queries versus dynamic queries. After further investigation, we found that this is indeed a plausible cause. In PyTorch, memory is managed through `cudaMalloc` and `cudaFree`, and this dynamic memory management approach could lead to frequent memory allocation calls in models like MOTR, where memory demand fluctuates. This could slow down the model and prevent full GPU utilization.

We experimented with PyTorch's memory management code, and observed that when the tensor size remains relatively constant, there are significantly fewer memory allocation and release calls. The specific code we tested can be easily found in GitHub, when you search for 'torch mem'(we would like to note that the owner of that link is not associated with the authors of this paper).

So how can we address this issue? Modifying PyTorch's underlying logic directly is quite complex and would likely require intervention from PyTorch's developers (we are preparing to submit an issue on GitHub or send an email to the maintainers). An alternative approach could be to fix the number of tracking queries in MOTR and use masks to differentiate between empty tracking queries and those that are actively used. This may resolve the issue. As shown in Figure 7, we trained an updated version of MOTR for one epoch on the DanceTrack dataset and tested the speed and GPU utilization. Due to limitations in funding, equipment, and time, we did not fully train the model to evaluate its performance. However, preliminary results show promise: after one epoch, the HOTA score on the validation set reached 18.5 and fps has increased from 16.5 to 25 with fp32 precision. Note that we have not reduced any network structure at this time. Interested readers are welcome to experiment with this approach themselves. It is relatively straightforward to implement, though we advise against using GPUs with less than 24GB of memory, as this may lead to out-of-memory errors.

Of course, this is just one possible explanation. Other factors may also contribute to the underutilization of GPU resources in MOTR-like models. If any readers have alternative insights, we welcome further discussion and collaboration.

C. Visualization of FastTrackTr Results

In this section, we will provide visualization results of our model on different datasets.

DanceTrack0022

DanceTrack0064

DanceTrack0100



Figure 8. Our model's visualization results on Dancetrack, where the same color represents the same object.

MOT17-01



MOT17-08



MOT17-14



Figure 9. Our model's visualization results on MOT17, where the same color represents the same object.

v_IUDUODIBSsc_c001



v_6OLCI-bhioc_c001



v_9MHDmAMx05I_c009

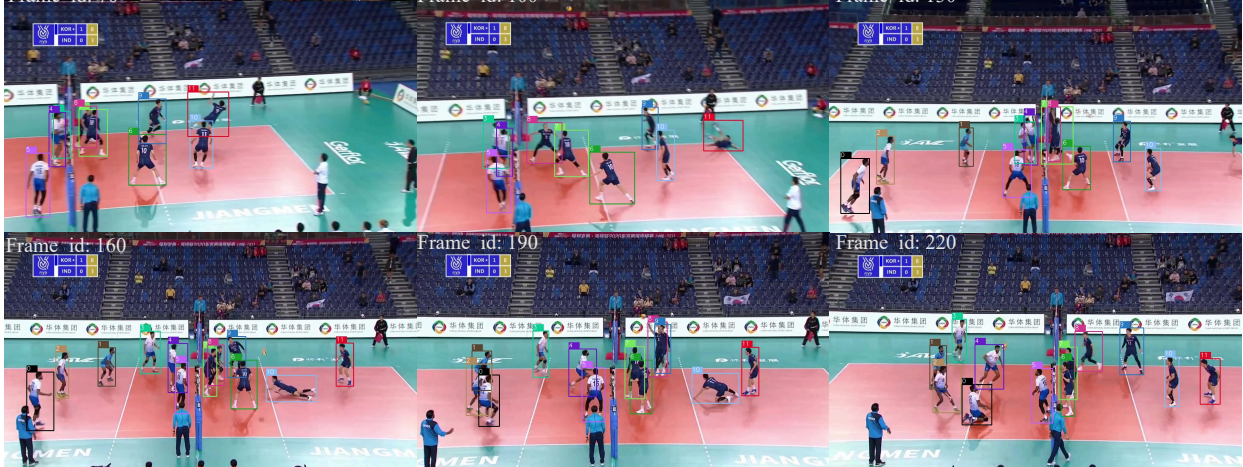


Figure 10. Our model's visualization results on SportsMOT, where the same color represents the same object.